15th Australasian Fluid Mechanics Conference
The University of Sydney, Sydney, Australia
13-17 December 2004

Numerical studies of contoured shock tube for murine powdered vaccine delivery system

Y. Liu*, N. K. Truong and M.A.F. Kendall

The PowderJect Centre for Gene and Drug Delivery Research
Department of Engineering Science, University of Oxford
Oxford OX2 6PE, United Kingdom
*Email:yi.liu@eng.ox.ac.uk

Abstract

A unique form of powdered delivery system, a biolistic system, has been developed. This novel technology is to accelerate particles in micro-particle form by a gas flow behind a travelling shock wave, so that they can attain sufficient momentum to penetrate the skin and thus achieve a pharmacological effect. One of the most recent developments is a mouse biolistic system, used in immunological studies. These studies require powdered vaccine to be delivered into the epidermis of the mouse with a narrow and highly controllable velocity distribution and a uniform spatial distribution. In this paper, Computational Fluid Dynamics (CFD) has been utilized to characterize the complete operation of a prototype mouse biolistic system. The key features of the gas dynamics and gas-particle interaction are discussed.

Introduction

A needle-free epidermal powdered delivery system, a biolistic system, has been developed at University of Oxford (Bellhouse et al, 1994, [1]). The underlying principle of the system is to accelerate a pre-measured dose of vaccine and drugs in microparticle form to an appropriate momentum by a high speed gas flow in order to penetrate the outer layer of the skin to achieve a pharmacological effect.

The biolistic system has shown many advantages over conventional needle and syringe, in terms of effectiveness, cost and health risk. The system can deliver powdered vaccine into a desired layer of skin or tissue to achieve the optimal effect. When antigenic compounds are delivered to skin or mucosa, the biolistic system requires less material to elicit the equivalent immune response [2, 12]. The formulation of vaccines in powder form can also improve stability, making transport and storage simple and inexpensive.

Recently, the mouse biolistic system, has been used in particle impact and immunological studies [7, 13, 14]. These studies require powdered vaccine preferably to be delivered into specific epidermis of the mouse skin with a narrow and controllable velocity range and uniform spatial distribution.

In this paper, Computational Fluid Dynamics (CFD) is utilized to simulate the gas and particle dynamics of a mouse biolistic system. The performance of this system is investigated in a series of numerical simulations. The main features of the starting process are presented. Predicted gas and particles characteristics within prototype system are compared with experimental data. The primary emphasis of this study is to gain new insights into the nozzle starting process and the interaction between the gas and particles. Representative results for a variant of the nozzle contour are given.

Murine biolistic system

Figure 1 shows a schematic of the mouse biolistic system, a variation of the Contoured Shock Tube system(CST). Key aspects of principles of operation are described by Kendall (see reference [6]). Essentially, the rupture of the diaphragms forms a primary shock wave, which propagates downstream and initiates an unsteady gas flow, as in a classical shock tube [15]. A quasi-state supersonic flow (QSSF) is subsequently established. In the course of these processes, particles are entrained in the gas flow and accelerated towards the nozzle exit. The gas is deflected, while the particles maintain a sufficient momentum to breach the stratum corneum and target the underlying cells in the viable epidermis.

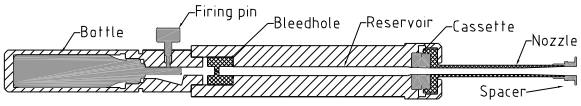

Figure 1: A schematic of the murine biolistics system.

The system is optimized such that the bulk of the particle cloud is accelerated in the QSSF and not in the starting process. This is achieved by the choice of system geometry, gas species, operation pressure and particles. The upstream termination boundary of the particle delivery window is defined by the reflected expansion wave. Therefore an emphasis is placed upon gaining new insights in to the nozzle starting process and the gas-particle interactions.

The characteristics of the steady flow generated by the prototype mouse biolistic system have been analyzed theoretically with ideal shock relations. For a nominal diaphragm burst pressure of 2070 *kPa*, the primary shock Mach number (Ma_s) is 2.343, the pressure for both Regions 2 and 3 in the shock tube is 632 *kPa*, and Mach numbers for Regions 2 and 3 (using standard shock tube nomenclature) are 1.133 and 0.787, respectively. The correctly expanded Mach number for helium at the nozzle exit is 2.11.

The CFD Model

In order to better understand the physical mechanics and help optimize the design, CFD is utilized to characterize the operation of the mouse biolistic system, illustrated in Figure 1.

For the solution, Fluent, a commercial available CFD software package [3], is employed to numerically simulate the multi-species gas flow and the interaction with the particles. Discrete and numerical solutions can be obtained by solving the governing partial differential equations (PDEs) using the finite volume method to determine the real gas flow field. The convective flux is discretized by an upwinding Roe vector difference splitter, and viscous term by the central difference. Time integration has been explicitly performed. Due to the unsteady motion of the shock wave process, a coupled explicit solver is chosen. An overall second order scheme is satisfied spatially and temporally. For an efficient, time-accurate solution of the preconditioned equations, a multi-stage scheme is employed.

Modelling of particle dynamics requires knowledge of the fluid flow field as well as the variation of the drag coefficient with relative Reynolds and Mach numbers. It is evident that there is great discrepancy between the correlations proposed for the particle drag coefficient. These discrepancies stem from the different ranges of Reynolds and Mach number covered, gas flows, particle sizes and density ranges and the particle concentration.

Regarding to our particular application, which consists of both subsonic and supersonic unsteady flow region, the correlation of Igra and Takayama [5], covering a wider range of Reynolds number (200 to 101,000), is implemented to determine the unsteady drag coefficient.

Some validation of this approach with prototypes of biolistic systems have been conducted through extensive comparison with experimental data [9, 10, 11] and computational results from the CFX calculations [4].

Results and discussion

The flow fields under consideration have circular cross sections and are assumed to be axisymmetric. The emphasis is on the events after diaphragm rupture, thus the gas filling process is not simulated. The diaphragm (shown in Figure 1) initially separates high-pressure driver gas (mixture of helium and air) and driven gas (air) at atmospheric pressure. In this study, a single diaphragm is assumed for simplicity, and no attempt is made to consider the effects of non-ideal diaphragm rupture. Similarly, we have not included the effects of tissue surface deformation, studied by Kendall et al [8]. The calculation is started with the instant rupture of the diaphragm when the driver mixture gas pressure reaches the pressure of 2.07 *MPa*, which has been approximately determined from the experiments.

Gas flow

The calculated and experimental history of the static pressure in the driver chamber (23 mm upstream of the diaphragm), is shown in Figure 2. The time zero is taken as the rupture of the diaphragm. The measured pressure is rather oscillatory and the level is higher than that CFD prediction. This discrepancy is attributed to the assumption of a closed gas filling system after diaphragm rupture, and perhaps a weak area change influence caused by the ruptured diaphragm and the unsteady expansion. This phenomenon is consistent with other biolistic systems [9, 4].

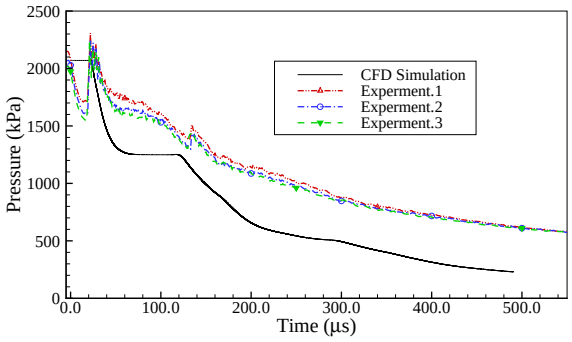

Figure 2: Calculated and measured pressure history.

In Figure 3, the simulated Pitot pressure history is compared with corresponding measurements from a centrally located Pitot probe of 3 *mm* downstream of the nozzle exit. The CFD has overestimated the Pitot pressure. This is largely due to poor spatial sensitivity of the probe in the supersonic flow (the diameter of the Pitot probe is about 2 *mm*, comparing with 4 *mm* of nozzle exit diameter), which is not considered in the simulation.

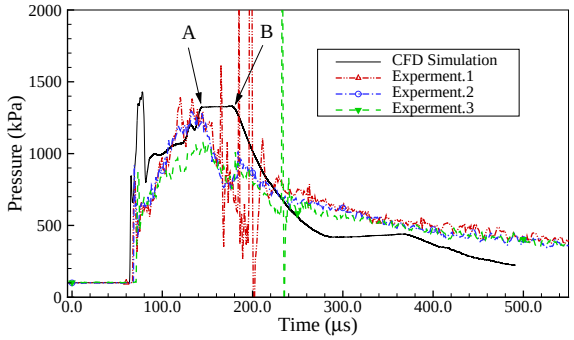

Figure 3: Calculated and measured Pitot pressure history.

In general, however, all the simulated pressure histories in Figure 2 and 3 are in good agreement with the measurements. The termination time of the starting process ("A" in Figure 3) is reasonable modelled. It demonstrates that shock, compression, expansion waves, and interactions between waves and the boundary layer are reasonably predicted by the numerical method employed.

Further investigation is obtained through examining the sequences of the flow field. Closer examination of the formation of the secondary shock is achieved at time of 89.3 μs and 107.4 μs after diaphragm rupture as shown in Figure 4.1 and 4.2. The contact surface between the primary shock and the secondary shock can be identified in the lower half of flow field. The contours within the QSSF, identified in Figure 3 to be 152.5 $\mu s.$, are shown in Figure 4.3.

Particle flow

The particle trajectories are advanced simultaneously with the generated gas flow field. In the calculation, the particles are assumed to be initially arranged in a matrix representing all the different possible positions within the vaccine particle cassette.

Figure 5 plots the calculated particle impact velocity as a function of radius. Particles were assumed as sphere with a density of 19,320 kg/m^3. The velocity plots clearly show that the particles are achieved velocity of approximately 640 m/s with a reasonably uniform.

Finally, the key gas flow regimes and the particles cloud trajectories are shown together in the calculated space-time (x-t) diagram, Figure 6. The representation of the gas flow is achieved by plotting the CFD calculation, in the typical form of contours of pressure. It can be seen that the particles have been accelerated to the nozzle exit, avoiding the starting process secondary shock and the reflected expansion wave, and thereby remaining in the quasi-steady supersonic flow (QSSF).

Alternative nozzle design

The other feature of Figure 6, illustrates oblique shocks associated with a weak overexpanded nozzle flow, and resulting separated flow. This observation leads to a new design of the supersonic nozzle to achieve a quasi-steady correctly expanded supersonic flow and a more uniform particle impact velocity. The results are present here.

Figure 7 shows the instantaneous velocity contours in the QSSF state obtained with an alternative,correctly expanded nozzle design. The uniformity of gas velocity distribution is further illustrated in Figure 8.

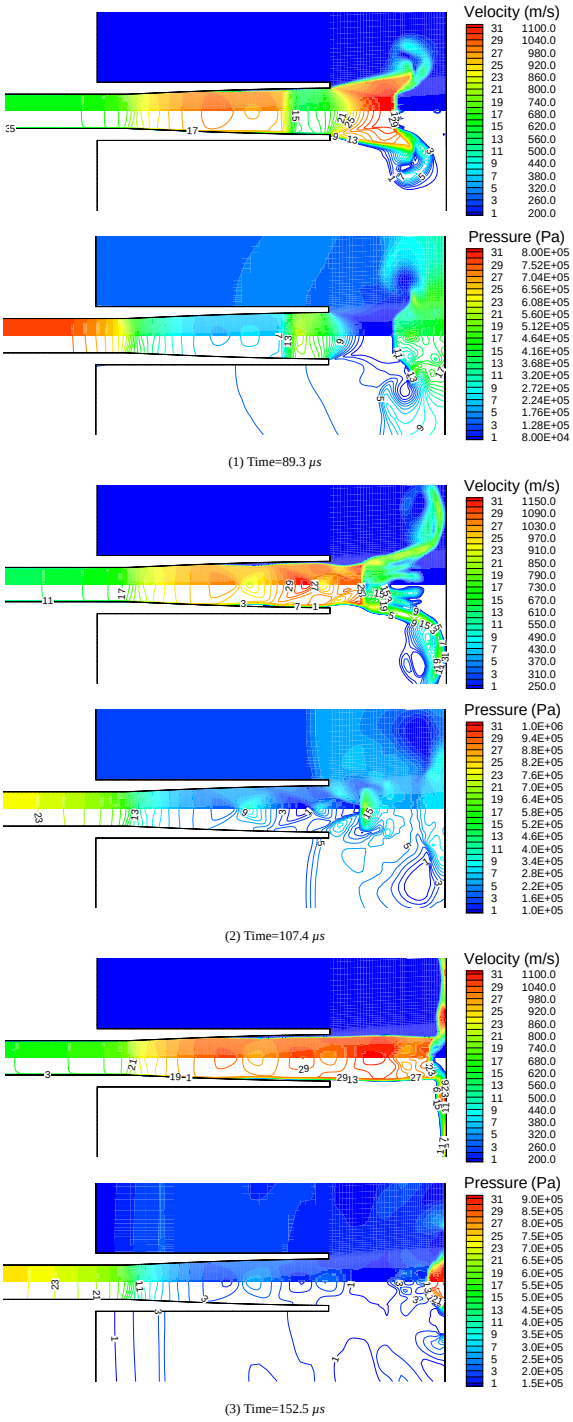

Figure 4: Instantaneous contour plots of velocity and pressure.

Figure 9 plots the calculated particle trajectories. The velocity plots clearly show that the particles are accelerated to a more uniform velocity. The improvement in impact velocity distribution is further illustrated by comparison with Figure 5. It is worthwhile to mention that the nozzle exit diameter has been reduced to 3.8 *mm*, still achieving a equivalent impact area. A statistic analysis of impact velocity, shown in Figure 10, provides 626 m/s of a mean velocity, with 1.61 m/s standard deviation.

Conclusions

A CFD model has been implemented to gain new insights into the mouse biolistic system used to accelerate vaccines in micro-

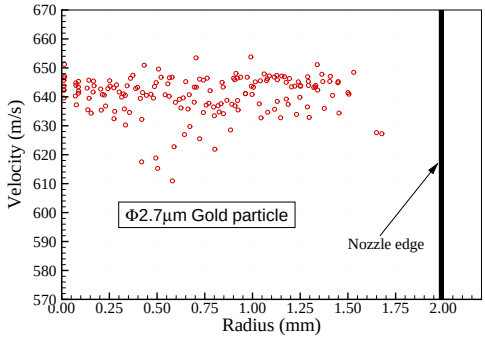

Figure 5: Calculated impact velocity of murine device.

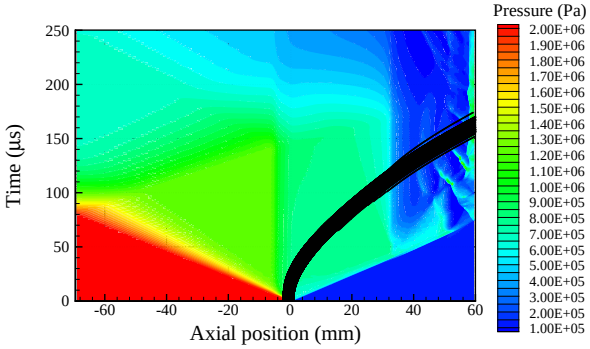

Figure 6: Constructed x-t characteristics from simulations.

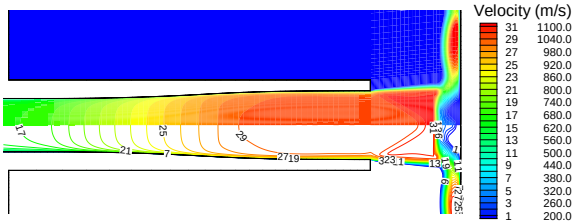

Figure 7: The Contour plot of velocity.

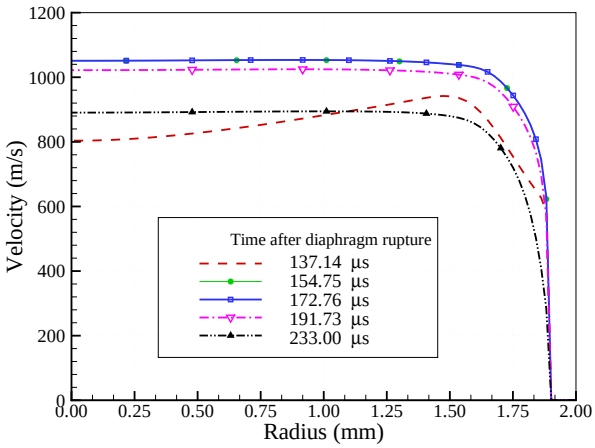

Figure 8: Velocity profiles along radius.

particle form to impart the skin. Fluent is utilized to simulate the unsteady gas flow and the interaction with the particles by a coupled explicit solver.

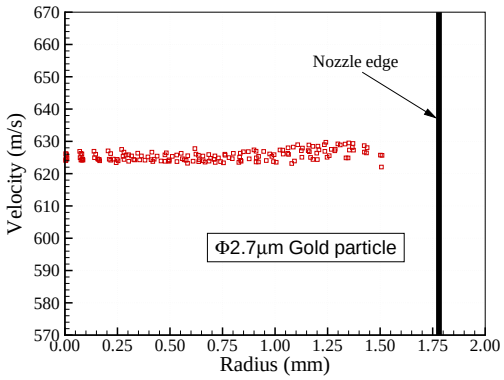

Figure 9: The impact velocity of new design murine device.

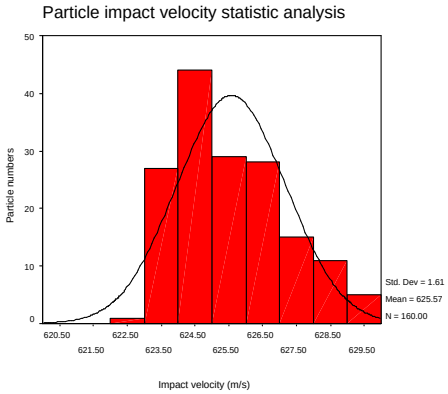

Figure 10: The statistic analysis of new design murine device.

Simulated pressure histories agree well with the corresponding static and Pitot pressure measurements. These calculations have been used to further explore the gas flow field, with an emphasis on the nozzle starting process. The quasi-steady supersonic flow window has been accordingly determined. The action of the gas flow in accelerating the particles was calculated within the modelled flow field. The main features of the gas dynamics and gas-particle interaction are presented.

The preliminary results demonstrate the overall capability of a new designed supersonic nozzle to deliver the particles to the skin targets with a more uniform velocity and spatial distribution.

Acknowledgements

The authors wish to thank professor B. J. Bellhouse, Powderject Centre for Gene and Drug Delivery Research, University of Oxford, for his encouragement of this work. This work was supported by PowderJect plc. and Chiron Vaccines. Their support is gratefully acknowledge.

References

[1] Bellhouse B.J., Sarphie D.F. and Greenford J.C., Needless syringe using supersonic gas flow for particle delivery. *Int. Patent WO94/24263.* 1994.

[2] Chen D.X., Endres R.L., Erickson C.A., Weis K.F., McGregor M.W., Kawaoka Y. and Payne1 L.G., Epidermal immunization by a needle-free powder delivery technology: Immunogenicity of influenza vaccine and protection in mice. *Nature Medicine* 2002, **(**6):1187–1190.

[3] Fluent user's guide volume, Fluent Inc. or see: http://www.fluent.com/.

[4] Hardy, M.P., Kendall, M.A.F., Quinlan, N.J. and Bellhouse, B.J., Numerical study of a prototype needle-free powdered vaccine delivery system. *Proc. 23nd Int. Symp. on Shock Waves, Austin, USA.* 2001.

[5] Igra, O., Takayama, K., Shock tube study of the drag coefficient of a sphere in a non-stationary flow. *Proc R. Soc. Land. A* 1993, **442**():231–2467.

[6] Kendall, M.A.F., The delivery of particulate vaccines and drugs to human skin with a practical, hand-held shock tube-based system. *Shock Waves Journal* 2002, **12**(1):22–30.

[7] Kendall M.A.F., Mulholland W.J., Tirlapur U.K., Arbuthnott E.S. and Armitage M., Targeted delivery of microparticles to epithelial cells for immunotherapy and vaccines: an experimental and probabilistic study, *The 6th International Conference on Cellular Engineering*, Sydney, Austrulia, 2003.

[8] Kendall M.A.F., Mitchell T.J., Hardy M.P. and De Focatiis D.S.A., Mucosal deformation from an impinging transonic gas jet and effects on biolistic particle impact velocity. *Submitted to Biomaterials Journal* 2004.

[9] Liu, Y., Kendall, M.A.F., Truong, N.K. and Bellhouse, B.J., Numerical and experimental analysis of a high speed needle-free powdered vaccines delivery device. AIAA-2002-2807. *Proc. 20th AIAA Applied Aerodynamics Conference, St. Louis, MO, USA.* 2002.

[10] Liu, Y., Kendall, M.A.F., Numerical simulation of heat transfer from a transonic jet impinging on skin for needle-free powdered drug and vaccine delivery. *Journal of Mechanical Engineering Science, Proceedings of the Institution of Mechanical Engineers Part C.* (Accepted on 15 July, 2004, Article in press)

[11] Liu, Y., Kendall, M.A.F., Numerical study of a transient gas and particle flow in a high-speed needle-free ballistic particulate vaccine delivery system. *Journal of Mechanics in Medicine and Biology* (Accepted on 7 May, 2004, Article in press)

[12] Loehr, B.I., Wilson, P., Babiuk, L.A. and S. van Drunen Little-van den Hurk Gene gun-mediated DNA immunization primes development of mucosal immunity against bovine herpes virus 1 in cattle, *J. Virol.* 2000,**74**:6077-6086.

[13] Mcsloy N.J., Raju P.A. and Kendall M.A.F., The effects of shock waves and particle penetration in skin on cell viability following gene gun Delivery. *1st British Society for Gene Therapy Conference*,Oxford, UK, 2004.

[14] Mitchell, T.J., Kendall, M.A.F. and Bellhouse, B.J. A ballistic study of micro-particle penetration to the oral mucosa, International *Journal of Impact Engineering* 2003, **28**(6): 581-599.

[15] Smith, C.E., The starting process in a hypersonic nozzle. *Joural of Fluid Mechanics* 1966, **24**(4):625–641.